ECCOMAS Congress 2016
VII European Congress on Computational Methods in Applied Sciences and Engineering
M. Papadrakakis, V. Papadopoulos, G. Stefanou, V. Plevris (eds.)
Crete Island, Greece, 5–10 June 2016

A FORCE-BASED FORMULATION FOR THE ANALYSIS OF 3-DIMENSIONAL INELASTIC STRUCTURAL FRAMES

Theodoros N. Patsios[1] **and Konstantinos V. Spiliopoulos**[2]

[1] Ph.D. Candidate, ISAAR, School of Civil Engineering, National Technical University of Athens
9 Heroon Polytechniou, Zografou Campus, 15780, Athens, Greece
e-mail: tpatsios@central.ntua.gr, tpatsios@gmail.com

[2] Professor, ISAAR, School of Civil Engineering, National Technical University of Athens
9 Heroon Polytechniou, Zografou Campus, 15780, Athens, Greece
e-mail: kvspilio@central.ntua.gr

Keywords: Force Method, 3D Frames, Plastic Hinges, Non-Holonomic Plasticity, Pushover Analysis.

Abstract. *A force-based formulation for the step-by-step non-linear (elastic-plastic) analysis of three-dimensional (3D) structural frames is presented. It uses the redundant force and moment components as primary unknowns, and approximates the non-linearity problem in an incremental pattern. Using a simple linear transformation, the equilibrium matrices are quickly formed via a partial multiplication of a subset of matrices with dimensions (3x3). The convex yield function that describes the static admissibility condition of each zero-length plastic hinge is approximated with a linear convex polyhedron (manifold), whose hyper plane equations are automatically defined with the help of De Bruijn sequences. In this way, a number of complex force/moment interaction criteria may easily be defined that take into account shear and torsion. Discontinuities (e.g. articulations) are also accounted for. Out of the partial derivatives of these yield functions with respect to the stresses, the corresponding plastic deformations are computed, with the help of Lagrange multipliers. The formulation may be solved using any non-linear optimization algorithm that solves for linear constraints. Results are compared to those of the equivalent direct stiffness method and to those of the existing literature, proving the efficiency of the proposed formulation.*

1 INTRODUCTION

In this paper, an existing step−by−step, force−based method [1] is further extended to the analysis of inelastic 3D structural frames. Techniques to define equilibrium matrices for incremental analysis have been already presented in [1], extending what was first presented in [2] for the case of optimal plastic design; remedies to these techniques in order to function for 3D structures were presented in [3].

Herein, an alternate linear transformation that requires fewer computer operations is introduced. Furthermore, a fully automated technique for generating any type of linearized yield function for up to six interacting stress components is developed, that is based on the assumption of lumped plasticity (*plastic hinge approach*). By definition, these generalized yield functions are able to also cater for shear and torsion, as well as for discontinuities (*e.g articulations*). The results are compared to those of widely accepted commercial packages and to those from the existing literature, proving the efficiency of the proposed formulation.

2 PROBLEM FORMULATION

2.1 Basic Equations

The force method is solely based on equilibrium arguments. For elastic analysis, an excellent review paper has been written by A. Kaveh [4]. The brief presentation that follows below incorporates plasticity.

The stress components of a structure may be represented by a vector "$\mathbf{Q_s}$" which is expressed as a linear combination of a vector "$\mathbf{Q_0}$" that contains a part of the stress components which is due to external loads and a vector "$\mathbf{Q_1}$" containing a part of the stress components which is due to internal redundant stresses; a load scaling factor "γ" may also be included:

$$\mathbf{Q_s} = \gamma \cdot \mathbf{Q_0} + \mathbf{Q_1} \tag{1}$$

The above equation may be further developed by expressing each of the two linearly independent vectors as the product of a matrix "$\mathbf{B_i}$" and a vector "$\mathbf{p_i}$", where $\mathbf{i}=\{0,1\}$. These matrices express the values of the stress components of the structure due to unit valued external loads "$\mathbf{p_0}$" and unit valued internal redundant stresses "$\mathbf{p_1}$", respectively:

$$\mathbf{Q_s} = \gamma \cdot \mathbf{B_0} \cdot \mathbf{p_0} + \mathbf{B_1} \cdot \mathbf{p_1} \tag{2}$$

Equation (2) may be satisfied for an infinite number of redundant stress vectors "$\mathbf{p_1}$", but the problem is narrowed down to a unique solution with the help of the compatibility condition, as was first proposed by James Clerk−Maxwell:

$$\mathbf{B_1^T} \cdot \mathbf{q_s} = \mathbf{0} \tag{3}$$

Where in (3), vector "$\mathbf{q_s}$" contains the generalized deformations of the actual structure at its points of reference (*nodes*), which may be expressed as the summation of their elastic "$\mathbf{q_{el}}$" and plastic "$\mathbf{q_{pl}}$" components:

$$\mathbf{q_s} = \mathbf{q_{el}} + \mathbf{q_{pl}} \tag{4}$$

The elastic components in (4) are computed with the help of the unassembled flexibility matrix "$\mathbf{F}$":

$$\mathbf{q_{el}} = \mathbf{F} \cdot \mathbf{Q_s} \tag{5}$$

The plastic components in (4) may be computed with the help of the axiom of maximization of plastic work [5], using the stress derivative of an adequately defined yield function "$g(\mathbf{Q_s})$":

$$\mathbf{q_{pl}} = \lambda \cdot \frac{\partial g(\mathbf{Q_s})}{\partial \mathbf{Q_s}} \tag{6}$$

Where in (6) "λ" denotes a Lagrange (*or plastic*) multiplier. This multiplier may be explicitly computed within the framework of mathematical programming [6], using a linear complementarity condition between the potential of the material to absorb stress up to its' conventional yield point (*plastic potential, or "Y_*"*), and the corresponding Lagrange (*plastic*) multiplier "λ":

$$\mathbf{Y}_*^T \cdot \boldsymbol{\lambda} = 0 \quad , \quad \mathbf{Y}_* \geq 0 \quad , \quad \boldsymbol{\lambda} \geq 0 \tag{7}$$

Schematically, the concept of the plastic potential "Y_*" and its' corresponding Lagrange (*plastic*) multiplier may be depicted in Figure 1 below:

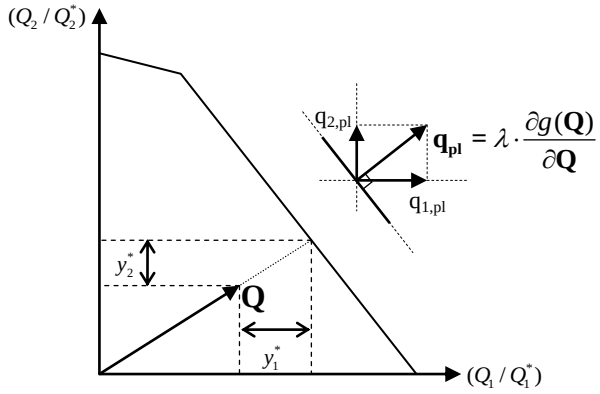

Figure 1: Plastic potential and corresponding Lagrange multiplier.

In algebraic terms, the plastic potential "Y_*" is a scalar, dimensionless quantity that expresses the numerical difference between the maximum and the actual value of the yield function, and is by definition nonnegative.

The displacements along the direction of the external loads may be computed with the help of the static−kinematic duality (SKD):

$$\mathbf{u} = \mathbf{B}_0^T \cdot \mathbf{q_s} \tag{8}$$

Historically, the SKD may be seen as another variant of the principle of virtual works (PVW), as was first proposed by Archimedes of Syracuse through the principle of leverage [7]; it expresses a "balance" between the work of external forces and the work of internal stresses that develop in the structure.

Another interesting remark is that the compatibility condition (3) may be seen as a special case of (8), where the displacements along the direction of the redundant components are zero.

2.2 Three-Dimensional Equilibrium

By considering the cross product in matrix form for a Cartesian space, the induced moments "**M**" at a particular point "*f*" due to a force vector "**F**" that is applied at another point "*s*" may be described by the following equation:

$$\mathbf{M} = \mathbf{d}_R \cdot \mathbf{F} = \left[\begin{array}{c|c|c} 0 & -\Delta z & +\Delta y \\ \hline +\Delta z & 0 & -\Delta x \\ \hline -\Delta y & +\Delta x & 0 \end{array}\right] \cdot \left\{\begin{array}{c} F_x \\ F_y \\ F_z \end{array}\right\} \tag{9}$$

Where

$$\Delta x = x_f - x_s \quad , \quad \Delta y = y_f - y_s \quad , \quad \Delta z = z_f - z_s \tag{10}$$

The equilibrium condition in global coordinates between the two points "*f*" and "*s*" may then be written in matrix form, as follows:

$$\left\{\begin{array}{c} \mathbf{F} \\ \mathbf{M} \end{array}\right\}_f = -\left[\begin{array}{cc} \mathbf{I} & 0 \\ \mathbf{d}_R & \mathbf{I} \end{array}\right] \cdot \left\{\begin{array}{c} \mathbf{F} \\ \mathbf{M} \end{array}\right\}_s \tag{11}$$

2.3 Linear Projections from Global to Local Coordinates

A simple to implement, yet efficient linear transformation from global to local coordinates, is the following:

$$\mathbf{v}_L = \mathbf{T}_R \cdot \mathbf{v}_G \tag{12}$$

Where $\mathbf{v}_G = \left\{ v_x \quad v_y \quad v_z \right\}^T$ is a vector whose components are defined with respect to a global Cartesian coordinate system with basis {x,y,z}, and $\mathbf{v}_L = \left\{ v_1 \quad v_2 \quad v_3 \right\}^T$ is the same vector with respect to a local Cartesian coordinate system with basis {1,2,3}. The transformation matrix "$\mathbf{T}_R$" for the general case may then be expressed as follows:

$$\mathbf{T}_R = \left[\begin{array}{c|c|c} +\dfrac{v_x}{L} & +\dfrac{v_y}{L} & +\dfrac{v_z}{L} \\ \hline -\dfrac{v_x}{L}\cdot\dfrac{v_z}{L_{xy}}\cdot\cos\alpha + \dfrac{v_y}{L}\cdot\sin\alpha & -\dfrac{v_y}{L}\cdot\dfrac{v_z}{L_{xy}}\cdot\cos\alpha - \dfrac{v_x}{L}\cdot\sin\alpha & +\dfrac{L_{xy}}{L}\cdot\cos\alpha \\ \hline +\dfrac{v_x}{L}\cdot\dfrac{v_z}{L_{xy}}\cdot\sin\alpha + \dfrac{v_y}{L}\cdot\cos\alpha & +\dfrac{v_y}{L}\cdot\dfrac{v_z}{L_{xy}}\cdot\sin\alpha - \dfrac{v_x}{L}\cdot\cos\alpha & -\dfrac{L_{xy}}{L}\cdot\sin\alpha \end{array}\right] \tag{13}$$

Where $L = \sqrt{{v_x}^2 + {v_y}^2 + {v_z}^2}$ and $L_{xy} = \sqrt{{v_x}^2 + {v_y}^2}$ and "α" is a rotation angle around the axis of the vector "$\mathbf{v}_G$", or "$\mathbf{v}_L$". This transformation is equivalent to the one presented in [3].

For each of the special cases where the global vector "$\mathbf{v}_G$" is perpendicular to a Cartesian plane {x,y} or {y,z} or {z,x}, the elements of the transformation matrix "$\mathbf{T}_R$" are efficiently defined using proper numerical exception handling workarounds with the help of the Levi−Civita cyclically interchanging index [8]. The rotation of angle "α" around the longitudinal axis is then applied separately, with the help of the corresponding (*rotation*) tensor "**R**":

$$\mathbf{R} = \left[\begin{array}{c|c|c} +1 & 0 & 0 \\ \hline 0 & +\cos\alpha & +\sin\alpha \\ \hline 0 & -\sin\alpha & +\cos\alpha \end{array}\right] \tag{14}$$

2.4 Equilibrium Matrices

The computation of the equilibrium matrices depends on the automated selection of a statically determinate basis that carries the external loads (*matrix* "$\mathbf{B_0}$") and of a minimal (*or near minimal*) cycle basis that defines the redundant stresses (*matrix* "$\mathbf{B}_1$"). These automation techniques rely on graph theory and algorithms; analytical presentations may be found in [1], [2] and [3].

From a computational implementation perspective, it is convenient to define the equilibrium matrices "$\mathbf{B_0}$" and "$\mathbf{B}_1$" using a set of pre−solved mathematical formulae that simultaneously express equilibrium in 3D space as well as transformation of the stress components from the global coordinate system to the local of each member of the structure. By combining equations (9) − (14), we have:

$$\mathbf{B}_i = \left[\begin{array}{c|c} \mathbf{T}_R & \mathbf{0}_{3x3} \\ \hline \mathbf{T}_R \cdot \mathbf{d}_R & \mathbf{T}_R \end{array}\right] \quad , \quad i = \{0,1\} \tag{15}$$

An additional (±) sign is to be applied to each row of (15), according to whether the direction of the local axes of the surface of the corresponding reference section coincide with the direction of the local axes of the corresponding member, or not.

In this way, the stress and the elastic and plastic strain components of each structural member for every step of the incremental procedure may be quickly evaluated, using the incremental forms of equations (2), (5) and (6), respectively.

2.5 Linearized Yield Functions

For an analysis of a structural frame that takes into account material post−elastic behavior, a plastic hinge approach is traditionally followed. From the strength of materials' point of view, the conventional limits between elastic and plastic deformations may be defined using a convex hull, which, in the case of the proposed method, is further approximated by a linear convex polyhedron (*also referred to as "manifold"*):

$$g(\mathbf{Q}) = \sum_{i=1}^{n} s_i \cdot \frac{Q_i}{(\pm) Q_i^*} \le c \tag{16}$$

Where $i=\{1,2,\ldots,n\}$, "n" is the number of stress components, $\mathbf{Q} = \{ N \quad Q_2 \quad Q_3 \quad T \quad M_2 \quad M_3 \}^T$ is a vector that contains all potentially interacting stress components (see Figure 2 below), and "*c*" is a dimensionless constant (e.g. *c*=1).

Figure 2: Local force and moment components at the end of a linear finite beam/column element.

Due to the 3-dimensional nature of the problem, a series of stress interaction criteria may be defined, e.g. $\{N,M_2,M_3\}$ or $\{T,M_2,M_3\}$ or $\{T,Q_2,Q_3\}$ or $\{N,Q_2,M_3\}$ or $\{N,Q_3,M_2\}$ or $\{N,Q_2,Q_3,M_2,M_3\}$, etc. Applied implementations of such criteria may be found e.g. in structural norms.

For example, the AISC−LRFD [9] proposes a criterion which is a bi-segmented yield function for bending moment and axial force interaction; schematically, it is presented in Figure 3 below:

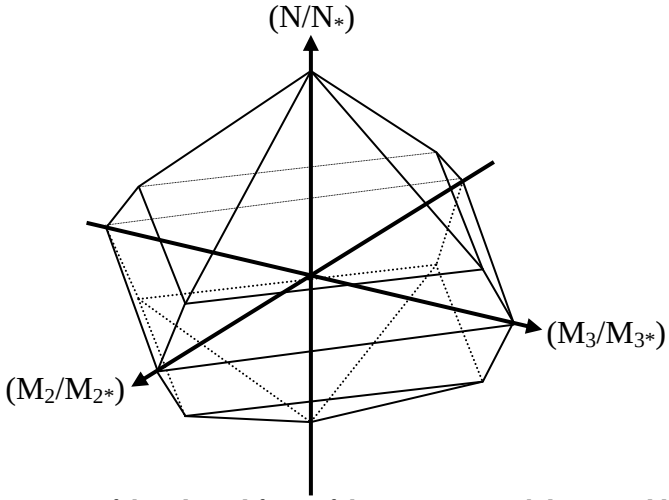

Figure 3: 3D illustration of the adopted form of the AISC-LRFD bilinear yield function.

Another example from engineering practice is the failure criterion according to DIN−18880, which is a multi−segmented yield function for bending moment, shear, and axial force interaction. A definition of this function for planar frames is analytically presented in [10]; herein, the corresponding coefficients for implementing this function according to (16) are summarized in Table 1 below:

S_i	N	Q	M
Eq. 1	−	−	1.00
Eq. 2	1.00	−	1.00/1.10
Eq. 3	−	0.45/1.15	1.00/1.15
Eq. 4	1.10/1.25	0.45/1.25	1.00/1.25
Eq. 5	−	1.00/0.90	−

Table 1: Coefficients "s_i" for the yield functions according to DIN-18800.

A practical problem that arises from the increase of the number of interacting components has to do with the (±) signs in (16), which are used to define the sector of the hyperspace wherein each one of the polyhedron's stress interaction hyper planes is located (*positive or negative plastic capacity for every stress component*); but this may be easily tackled with the help of De Bruijn sequences [11].

For example, consider the simplest case of two interacting stress components (n=2), where sets of two are formed from the alphabet with symbols {+,−} (q=2). Then, we have four possible sets ($q^n=2^2=4$) which form one distinct sequence ($B=(2!)^{2^{2-1}}/2^2=1$), shown in Figure 4:

$$\{+,+\},\{+,-\},\{-,+\},\{-,-\}$$

Figure 4: De Bruijn sequence for the signs of a yield function with two interacting components.

Next, consider the case of three interacting components (n=3) where sets of three are formed from the alphabet with symbols {+,−} (q=2). Then, we have eight possible sets ($q^n=2^3=8$) which form two distinct sequences ($B=(2!)^{2^{3-1}}/2^3=2$), shown in Figure 5:

$$\{+,+,+\},\{+,+,-\},\{+,-,+\},\{+,-,-\}$$
$$\{-,+,+\},\{-,+,-\},\{-,-,+\},\{-,-,-\}$$

Figure 5: De Bruijn sequences for the signs of a yield function with three interacting components.

It may be observed in Figure 5 above, that one sequence is a negated permutation of the other; in fact, the sequence consists of the sequence shown in Figure 4, embedded in a simple (*elementary*) set (of n=1 and q=2). This means, that, using the sequence of Figure 4 as a basis, and in combination with the basic principle of enumeration, all possible sequences may be constructed following the same pattern of successive embedding (*or concatenation*).

A last example follows below, where five interacting components (n=5) are forming sets of five from the alphabet with symbols {+,−} (q=2), yielding a total of thirty two sets ($q^n=2^5=32$) which form potentially two thousand and forty eight sequences ($B=(2!)^{2^{5-1}}/2^5=2048$); one of these has been formed using the aforementioned successive embedding (*concatenation*) technique, and is schematically presented in Figure 6:

$$\{+,+,+,+,+\},\{+,+,+,+,-\},\{+,+,+,-,+\},\{+,+,+,-,-\}$$
$$\{+,+,-,+,+\},\{+,+,-,+,-\},\{+,+,-,-,+\},\{+,+,-,-,-\}$$
$$\{+,-,+,+,+\},\{+,-,+,+,-\},\{+,-,+,-,+\},\{+,-,+,-,-\}$$
$$\{+,-,-,+,+\},\{+,-,-,+,-\},\{+,-,-,-,+\},\{+,-,-,-,-\}$$
$$\{-,+,+,+,+\},\{-,+,+,+,-\},\{-,+,+,-,+\},\{-,+,+,-,-\}$$
$$\{-,+,-,+,+\},\{-,+,-,+,-\},\{-,+,-,-,+\},\{-,+,-,-,-\}$$
$$\{-,-,+,+,+\},\{-,-,+,+,-\},\{-,-,+,-,+\},\{-,-,+,-,-\}$$
$$\{-,-,-,+,+\},\{-,-,-,+,-\},\{-,-,-,-,+\},\{-,-,-,-,-\}$$

Figure 6: De Bruijn sequences for the signs of a yield function with five interacting components.

In practice, only one of these 2048 sequences is required in order to properly describe all the hyper planes of the polyhedron (*manifold*), since, by definition, all other sequences are only permutations of the sets of five that form the initial sequence.

Sequences for the case of alphabets with two elements were first proved by Camille Flye Sainte−Marie [12], 24 years before Nicolaas Govert de Bruijn was born.

2.6 Implementation of Discontinuities

For the case of sections that include discontinuities (*e.g. articulations*), a disjunction of the interacting components of the corresponding plastic hinge may be imposed that allows plasticization only for the active stress component(s).

For example, consider an articulated beam element with plastic hinges according to the AISC−LRFD criterion, defined for {N,M_2,M_3} interaction. Since the element has articulations at both of its' ends, the {M_2} and {M_3} components will be always zero, for both positive and negative rotations; this leaves only the {N} component as active candidate for plasticization. In practice, this means that a separate static admissibility condition for each stress component must be defined; thus, we will have a yield function consisting of three separate parts, one for each component, with the formulae for {M_2} and {M_3} being degenerate, in order to describe that the corresponding bearing capacity is zero. This disjunct yield function is presented in equation (17):

$$\begin{aligned} g_1(\mathbf{Q}) &= \left\{ \tfrac{1}{(\pm)N^*} \quad 0 \quad 0 \quad 0 \quad 0 \quad 0 \right\} \cdot \mathbf{Q} \le 1 \\ g_2(\mathbf{Q}) &= \left\{ 0 \quad 0 \quad 0 \quad 0 \quad \pm 1 \quad 0 \right\} \cdot \mathbf{Q} \le 0 \\ g_3(\mathbf{Q}) &= \left\{ 0 \quad 0 \quad 0 \quad 0 \quad 0 \quad \pm 1 \right\} \cdot \mathbf{Q} \le 0 \end{aligned} \tag{17}$$

Where $\mathbf{Q}=\{ N \quad Q_2 \quad Q_3 \quad T \quad M_2 \quad M_3 \}^T$ is the stress vector of the corresponding critical section and the (±) sign is used to denote upper and lower bounds.

It should be noted that the proposed disjunction technique presented in (17) may be used to define all sorts of discontinuities; the corresponding Lagrange multiplier is added to its' elastic counterpart in order to yield the actual elastic generalized displacement of the corresponding discontinuity.

2.7 Problem Formulation

By combining equations (2), (15) and (16), the yield function "$g(\mathbf{Q})$" may be explicitly expressed as a function of the external loads and the redundant stresses. By packing the coefficients of this composite function into an incidence matrix "$\mathbf{N}$", a linear constraint inequality may be established:

$$\mathbf{Y}_* = \mathbf{c} - \left(\mathbf{N}^T \cdot \mathbf{B}_1\right) \cdot \mathbf{p}_1 - \gamma \cdot \left(\mathbf{N}^T \cdot \mathbf{B}_0\right) \cdot \mathbf{p}_0 \geq \mathbf{0} \tag{18}$$

By substituting equation (2) into (5), then evaluating (6) with the help of (16), then substituting both into (4) and then into (3), the first derivative of a Lagrange function is obtained:

$$\left(\mathbf{B}_1^T \cdot \mathbf{F} \cdot \mathbf{B}_1\right) \cdot \mathbf{p}_1 + \gamma \cdot \left(\mathbf{B}_1^T \cdot \mathbf{F} \cdot \mathbf{B}_0\right) \cdot \mathbf{p}_0 + \left(\mathbf{B}_1^T \cdot \mathbf{N}\right) \cdot \boldsymbol{\lambda} = \mathbf{0} \tag{19}$$

Equations (18) and (19) together with (7) may be seen as the Karush−Kuhn−Tucker (KKT) conditions of the following optimization problem:

$$\begin{aligned} \textit{Min.}: \quad & f(\mathbf{p}_1) = \frac{1}{2} \cdot \mathbf{p}_1^T \cdot \left(\mathbf{B}_1^T \cdot \mathbf{F} \cdot \mathbf{B}_1\right) \cdot \mathbf{p}_1 + \gamma \cdot \mathbf{p}_1^T \cdot \left(\mathbf{B}_1^T \cdot \mathbf{F} \cdot \mathbf{B}_0\right) \cdot \mathbf{p}_0 \\ \textit{s.t.} \quad & \left(\mathbf{N}^T \cdot \mathbf{B}_1\right) \cdot \mathbf{p}_1 \leq \mathbf{c} - \gamma \cdot \left(\mathbf{N}^T \cdot \mathbf{B}_0\right) \cdot \mathbf{p}_0 \end{aligned} \tag{20}$$

In order to efficiently trace all the plasticization events along any given loading path, the independent variables and the critical parameters stated in the problem of equation (20) are replaced by their corresponding increments:

$$\begin{aligned} \textit{Min.}: \quad & f(\Delta\mathbf{p}_{1,k}) = \frac{1}{2} \cdot \Delta\mathbf{p}_{1,k}^T \cdot \left(\mathbf{B}_1^T \cdot \mathbf{F} \cdot \mathbf{B}_1\right) \cdot \Delta\mathbf{p}_{1,k} + \Delta\gamma \cdot \Delta\mathbf{p}_{1,k}^T \cdot \left(\mathbf{B}_1^T \cdot \mathbf{F} \cdot \mathbf{B}_0\right) \cdot \Delta\mathbf{p}_{0,k} \\ \textit{s.t.} \quad & \left(\mathbf{N}^T \cdot \mathbf{B}_1\right) \cdot \Delta\mathbf{p}_{1,k} \leq \mathbf{c}_k - \mathbf{Q}_{k-1} - \Delta\gamma \cdot \left(\mathbf{N}^T \cdot \mathbf{B}_0\right) \cdot \Delta\mathbf{p}_{0,k} \end{aligned} \tag{21}$$

Where in (21) "k" is the step's counter. The problem is solved in an incremental pattern using any efficient algorithm (e.g. [13], [14]); a detailed description of the adopted numerical strategy may be found in [1].

3 EXAMPLES

In the following context, four indicative examples are presented in order to verify the functionality of the proposed force−based formulation. Where possible, results are quantitatively compared with those of a widely accepted commercial program that uses the equivalent direct stiffness method; where not, with results according to methods found in the literature.

3.1 1 Storey, 1 Bay, Eccentric Braced 3D Frame

A single-storey, single-bay, eccentric-braced frame is used as a first test example to prove the efficiency of the proposed formulation. The frame's height is H=3m, and distances between columns are L_x=L_y=6m. All columns are placed so that their strong bending axis is parallel to the y-axis of the global coordinate system, and are fully fixed at the basis. Beams are placed so that they bend along their strong axis due to external forces applied along the z-axis, and are subdivided into smaller elements of length L=0.6m each. The braces are placed inside the openings which are parallel to the y-z plane, are assumed articulated at both of their ends, and are load-free. Schematically, the frame is illustrated in Figure 7:

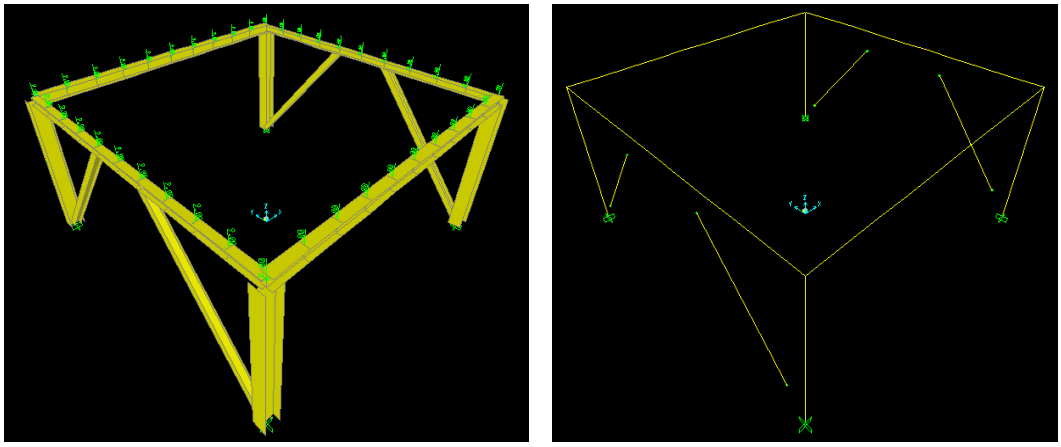

Figure 7: 3D illustrations of the 1−storey 1−bay, eccentric−braced frame (snapshots from SAP2000).

The frame's definitions (*nodal numbering & coordinates, member connectivity, section assignments and interacting stress components*) are summarized in Tables 2 and 3:

Node	x	y	z	Node	x	y	z
1	6.00	6.00	0.00	7	0.00	3.60	3.00
2	0.00	6.00	0.00	8	0.00	2.40	3.00
3	0.00	0.00	0.00	9	0.00	0.00	3.00
4	6.00	0.00	0.00	10	6.00	0.00	3.00
5	6.00	6.00	3.00	11	6.00	2.40	3.00
6	0.00	6.00	3.00	12	6.00	3.60	3.00

Table 2: Nodal coordinates of the 1−storey 1−bay, eccentric−braced frame.

Member	Node: Start → End	Section	Interacting Components	Member	Node: Start → End	Section	Interacting Components
1	1 → 5	HEM260	{N,M2,M3}	9	6 → 5	HEM180	{M2,M3}
2	2 → 6	HEM260	{N,M2,M3}	10	9 → 8	HEB140	{M2,M3}
3	3 → 9	HEM260	{N,M2,M3}	11	8 → 7	HEB140	{M2,M3}
4	4 → 10	HEM260	{N,M2,M3}	12	7 → 6	HEB140	{M2,M3}
5	1 → 12	HEB140	{N,M2,M3}	13	9 → 10	HEM180	{M2,M3}
6	2 → 7	HEB140	{N,M2,M3}	14	10 → 11	HEB140	{M2,M3}
7	3 → 8	HEB140	{N,M2,M3}	15	11 → 12	HEB140	{M2,M3}
8	4 → 11	HEB140	{N,M2,M3}	16	12 → 5	HEB140	{M2,M3}

Table 3: Connectivity, sections, and interacting components of the 1−storey 1−bay, eccentric−braced frame.

The material of the structure is S235, with a Young's Modulus E=2.0E+8kPa, a conventional yield stress of f_y=235MPa, and is considered to be elastic-perfectly plastic.

To simulate material non−linearity, the concentrated plasticity approach is followed. For the columns, the bilinear AISC−LRFD criterion is used [9], for $\{N,M_2,M_3\}$ interaction. For the beams, the coupled bending moment $\{M_2,M_3\}$ variant of the same criterion is applied, without the participation of the axial forces {N}; in order to be able to compare with SAP2000, the effect of torsion {T} on beams was purposefully left out, since no torsion-bending interaction is supported by the available version of the program [15]. A linear relation between $\{M_2\}$ and $\{M_3\}$ was adopted for both interaction criteria. Articulations at the ends of the braces were implemented according to equation (17).

All beams are subject to a uniform load of 15kN/m. Each beam is divided into smaller elements of 0.6m length, and uniform loads are converted into a finite set of equally sized point loads of 9kN. Lateral loads are applied to the four top-corner nodes of the frame.

Two pushover analyses were run, one for each horizontal direction {x,y}. The base shear vs. roof displacement curves of the structure are presented in Figures 8 and 9 below, where quantitative comparisons with SAP2000 [15] are also included; for SAP2000, default analysis parameters were used.

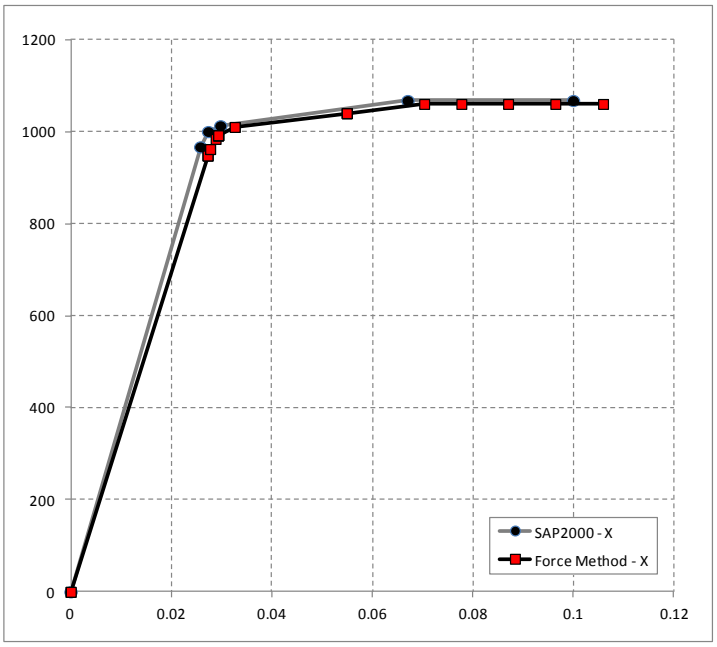

Figure 8: Pushover curve of the 1−storey, 1−bay, eccentric−braced frame; X−Direction; Units: {kN,m}.

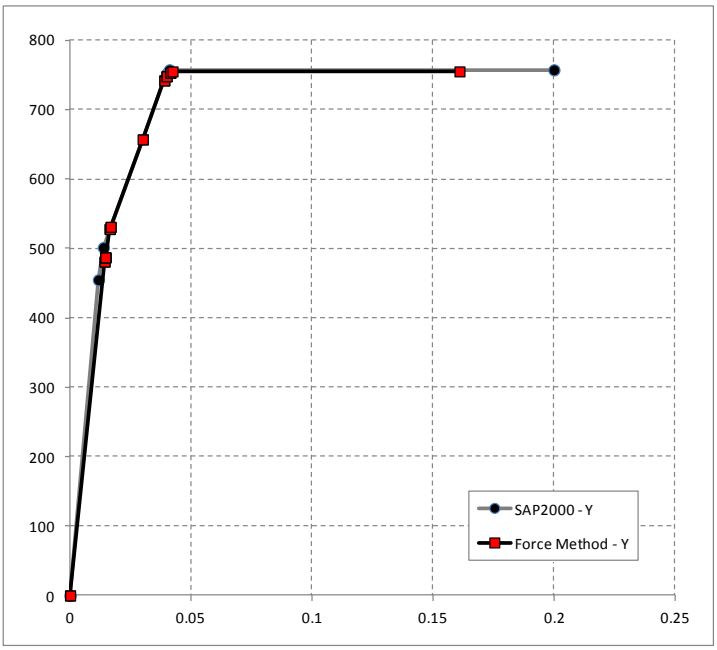

Figure 9: Pushover curve of the 1−storey, 1−bay, eccentric−braced frame; Y−Direction; Units: {kN,m}.

As it may be seen, results are in good accordance; the ultimate base shear is $V_{b,x}$~1067kN for the x-direction, and $V_{b,y}$~757kN for the y-direction.

3.2 6 Storey, 1 Bay, 3D Frame

A six-storey frame, with one-bay at each horizontal direction, is used as a second test example to prove the efficiency of the proposed formulation. Each storey has a height H=3.0m and each bay an opening L_x=L_y=6.0m. Beams are subdivided into smaller elements of length L=0.6m each; columns are placed so that their strong bending axis is parallel to the y-axis, and are fully fixed at the basis. The geometry of the frame is illustrated in Figure 10 below:

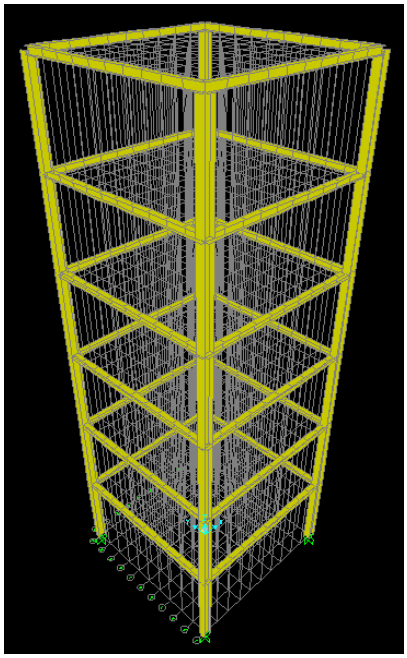

Figure 10: 3D illustration of the 6−storey frame (snapshot from SAP2000).

The sections of beams and columns were purposefully selected in order to form a strong column−weak beam sway mechanism, and are summarized in Table 4 below:

Members	Length	Section	Material
Columns	3.0m	HEM300	S235
Beams	6.0m	HEM180	S235

Table 4: Section properties of the six storey frame.

The material of the structure is S235, with a Young's Modulus E=2.0E+8kPa, a conventional yield stress of f_y=235MPa, and is considered to be elastic-perfectly plastic.

To simulate material non−linearity, the concentrated plasticity approach is followed, according to the exact assumptions that were made for the first example.

All beams are subject to a uniform vertical load of 15kN/m. Each beam is subdivided into ten smaller elements of length L=0.6m each, and the distributed loads are converted into a finite set of equally sized point loads of value 9kN each.

A lateral load pattern is applied to the beam−column junction nodes. The load distribution is defined as linearly varying with respect to the height of each storey (*1st eigenmode, with 100% participation*).

Two pushover analyses were run, one each horizontal direction (x,y). The base shear vs. roof displacement curves of the structure is presented in Figures 11 and 12 below, where a quantitative comparisons with SAP2000 [15] are also included; for SAP2000, default analysis parameters were used.

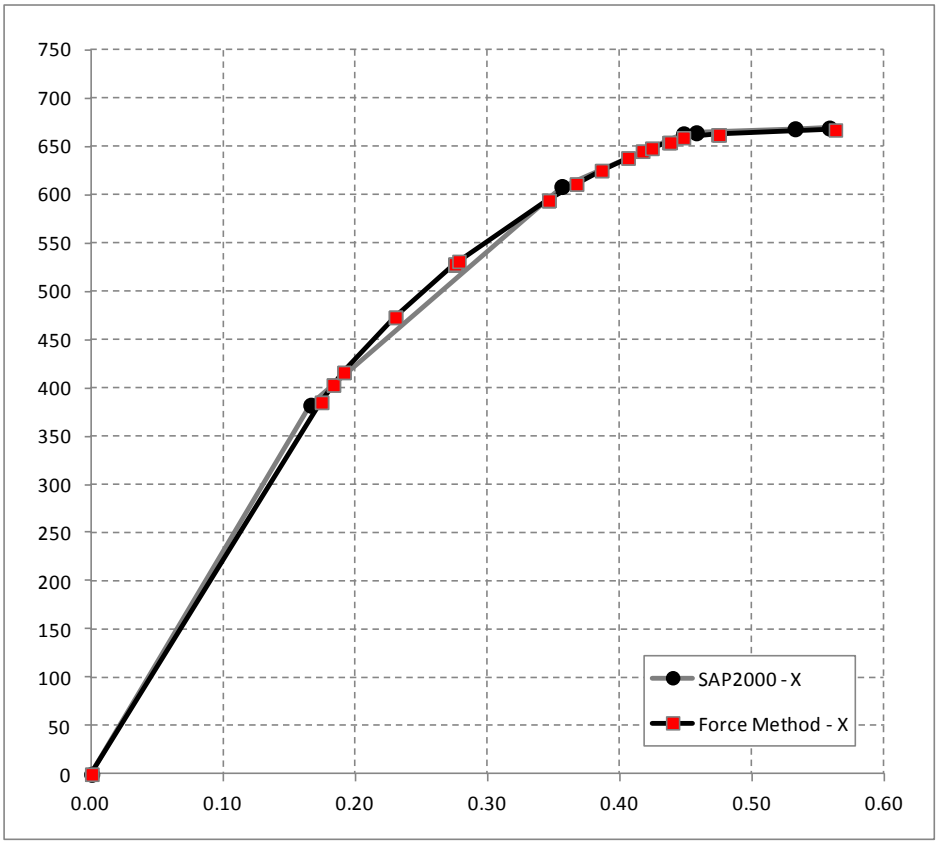

Figure 11: Pushover curves of the six−storey frame, x−direction; Units: {kN,m}.

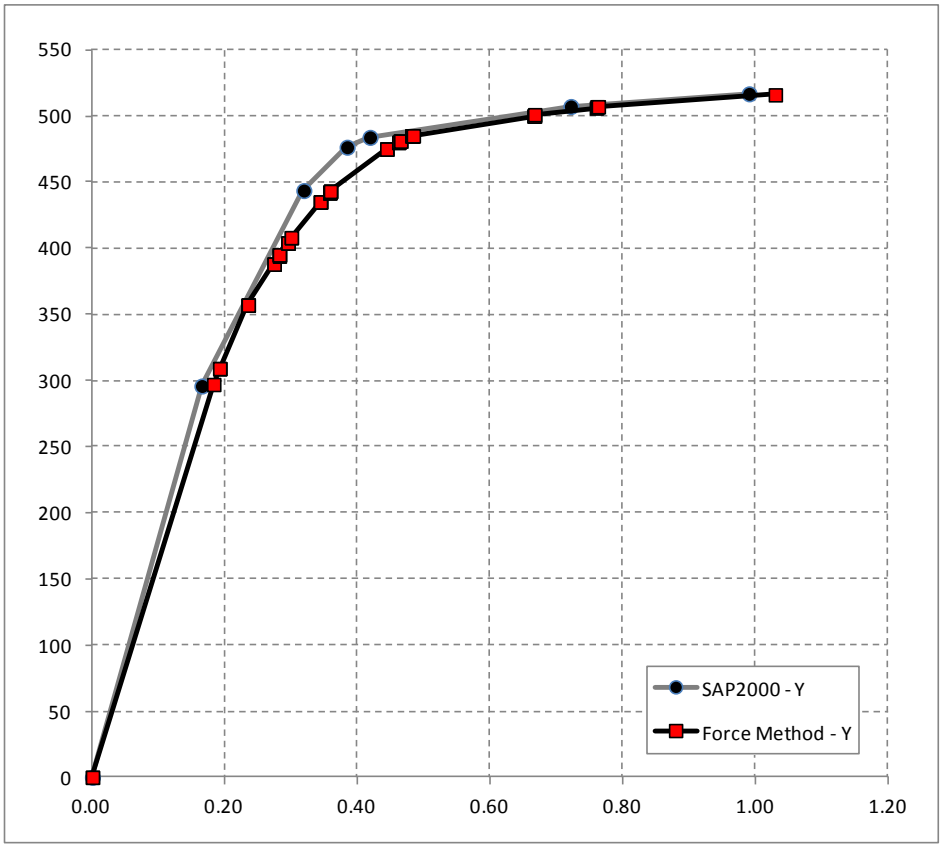

Figure 12: Pushover curves of the six−storey frame, y−direction; Units: {kN,m}.

As it may be seen, the results are in good accordance; the ultimate base shear along the x-direction is $V_{b,x}$~667kN, and along the y-direction is $V_{b,y}$~516kN.

3.3 1 Storey, 1 Bay, Portal 2D Frame

This example is used to test the functionality of the herein implemented yield function according to DIN−18800, via a comparison with AISC−LRFD; to this extend, I-beams are used.

The frame's height is H=3.0m and length L=6.0m. The beam's section is HEB160 and the columns' sections are HEM200. All structural elements are placed so as to bend around their strong axis. The beams are subdivided into smaller elements of length L=0.6m each. Columns are fully fixed at the basis. Schematically, the portal frame may be seen in Figure 13 below:

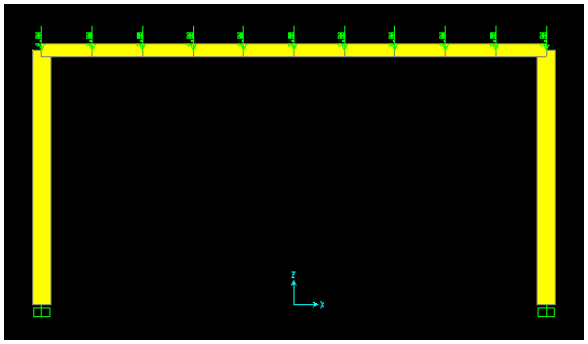

Figure 13: Geometry of the portal frame and vertical loads (snapshot from SAP2000).

The material of the structure is S235 with a Young's Modulus E=2.0E+8kPa, a conventional yield stress of f_y=235MPa, and is considered to be elastic-perfectly plastic.

A uniform vertical load of magnitude 15kN/m is applied to the beam, which is simulated by finite point loads of magnitude 9kN each, applied in equal distances of 0.6 m. A horizontal force is applied to the top left node.

Two pushover analyses were performed using the proposed formulation; one using the AISC−LRFD yield function and one using the DIN−18800. The results were compared to those of SAP2000 [15] and were found in good accordance. All base shear vs. roof displacement curves are plotted in Figure 14 below:

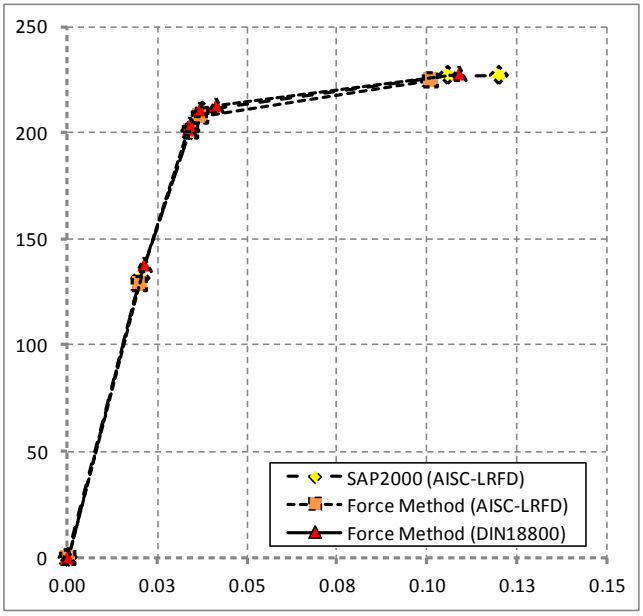

Figure 14: Pushover curves of the 2D portal frame; Units: {kN,m}.

3.4 A Simple Grillage

This simple example is used to demonstrate the functionality of the proposed formulation for structures where the contribution of torsion is important. Grillages are a typical case; a simple grillage found in [16] is used as reference. Schematically, it is presented in Figure 15:

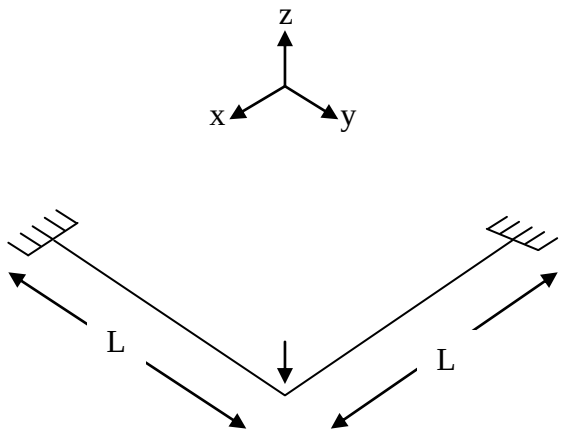

Figure 15: Geometry and loading of the grillage.

As it may be observed, the geometrical proportions and loading conditions are the same as in [16]; herein, elements have a length L=3m and a rectangular tube section with dimensions (bxh)=(160x160)mm and thickness t=10mm.

The material of the structure is S235 with a Young's Modulus E=2.0E+8kPa, a conventional yield stress of f_y=235MPa, and (*of course*) is considered to be elastic-perfectly plastic.

Additionally to the assumptions above, the yield locus was linearized so as to be in accordance with the proposed formulation. An analytical derivation of the collapse load according to the linear yield function adopted follows below:

$$g(T, M_3) = \frac{T}{T_p} + \frac{M_3}{M_{3,p}} - 1 \le 0 \tag{22}$$

The partial derivatives of the yield function with respect to each stress component are:

$$\frac{\partial g}{\partial T} = \frac{1}{T_p} \quad , \quad \frac{\partial g}{\partial M_3} = \frac{1}{M_{3,p}} \tag{23}$$

Thus, with the help of (23), the ratio of bending (θ) to torsion (γ) plastic rotations will be:

$$\frac{\theta}{\gamma} = \left(\frac{T_p}{M_{3,p}} \right) \cdot \frac{M_3}{T} \tag{24}$$

As also stated in [16], a plastic bending rotation in the proximity of a support node of one beam will result in an equal rotation due to torsion in the other beam, in the proximity of the connection node between the two elements. Thus, from (24) we infer the following linear proportion:

$$\frac{M_3}{M_{3,p}} = \frac{T}{T_p} \tag{25}$$

According to [16], the equation that gives the collapse load is the following:

$$\frac{1}{2} \cdot P \cdot L = M_3 + T \tag{26}$$

By combining (25) and (26), and by assuming for simplicity that $M_{3p}=T_p$, we have:

$$P_C = \frac{2 \cdot M_{3,p}}{L} \tag{26}$$

For the selected cross-section and material, $M_{3p}=79.4kNm$; thus, from (26), P_C=52.93kN.

An analysis using the proposed incremental formulation of (21) was run, and the resulting load vs. corresponding displacement curve is presented in Figure 16 below:

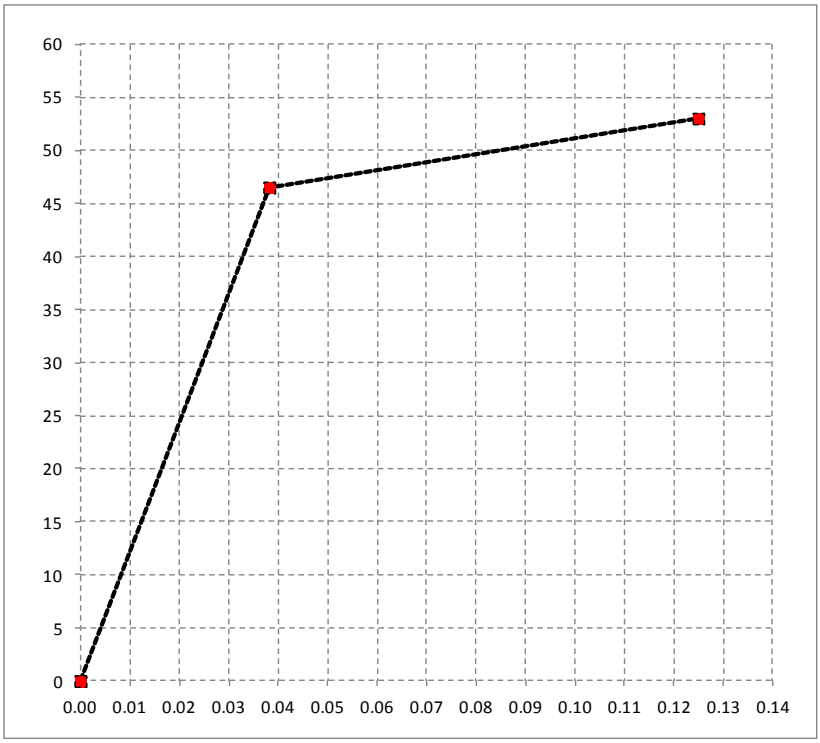

Figure 16: Load vs. corresponding displacement curve of the grillage; Units: {kN,m}.

As it may be seen, the results are in good accordance; the collapse load according to the proposed method is P_C~53kN.

4 CONCLUDING REMARKS

- The proposed formulation has good convergence properties and yields good results, even for relatively large scale problems. However, an implementation using a solver suitable for sparse matrices is required, in order to drastically reduce the CPU time.
- Non−holonomic plasticity is taken into account following a stepwise holonomic approach that is natively contained into the problem's formulation; no particular numerical remedies are required.
- Treatment of the effect of shear and torsion is also natively accommodated; however, it should be noted, that, when using the lumped plasticity approach, the warping stresses according to Vlasov [17] may be taken efficiently into account only in certain cases with the introduction of additional stress components, the bi−moments, which are defined as self−equilibrating systems on a section level.
- P−Δ effects and large displacements [18], material hardening [19] and softening, may also be included.

ACKNOWLEDGMENTS

The authors would like to thank Dimitra Voukia, M.Sc. Civil Engineer, for kindly providing us with a copy of [10].

REFERENCES

[1] K.V. Spiliopoulos, T.N. Patsios, An efficient mathematical programming method for the elastoplastic analysis of frames, *Engineering Structures*, **32** (5), 1199-1214, 2010.

[2] Spiliopoulos, K.V.. On the automation of the force method in the optimal plastic design of frames. *Computer Methods in Applied Mechanics and Engineering*, **141** (1–2), 141–156, 1997.

[3] K.V. Spiliopoulos, N.G. Dais, A powerful force-based approach for the limit analysis of three-dimensional frames. *Archive of Applied Mechanics*, **83** (5), 723–742, 2012.

[4] A.Kaveh, Recent Developments in the Force Method of Structural Analysis. *Applied Mechanics Reviews*, **45** (9), 401–418, 1992.

[5] R.O. Davis, A.P.S. Selvadurai, *Plasticity and Geomechanics*, Cambridge University Press, 2002.

[6] G. Maier, Quadratic programming and theory of elastic-perfectly plastic structures, *Meccanica*, **3** (4), 265–273, 1968.

[7] D. Capecchi, *History of Virtual Work Laws: A History of Mechanics Prospective*, Springer-Verlag, Italy, 2012.

[8] I. Vardoulakis, *Lecture Notes in Continuum Mechanics*, NTUA, 2008.

[9] *Load and resistance factor design specification for structural steel buildings, 2nd Edition*. Chicago: American Institute of Steel Construction; 1993.

[10] N. Gebbeken, *Eine Fliessgelenktheorie Höherer Ordnung für Raümliche Stabtragwerke*, Mitteilungen des Institus für Statik der Universität Hannover, Hannover, 1988.

[11] N.G. de Bruijn, A combinatorial problem, *Proc. Koninklijke Nederlandse Akademie v. Wetenschappen*, **49** (7), 758–764, 1946.

[12] Flye Sainte-Marie, C., Solution to question nr. 48, *L'intermédiaire des Mathématiciens*, **1**, 107–110, 1894.

[13] D. Goldfarb, A. Idnani, A numerically stable dual method for solving strictly convex quadratic programs, *Mathematical Programming*, **27**, 1–33, 1983.

[14] M.J.D. Powell, *TOLMIN: A Fortran Package for Linearly Constrained Optimization Calculation*, DAMTP, 1989/NA2, Cambridge, 1989.

[15] SAP2000, v14.0.0. User's manual. CSI Inc. 2009.

[16] J. Heyman, *Elements of the Theory of Structures*, Cambridge University Press, 1996.

[17] V.Z. Vlasov, *Thin-Walled Elastic Beams*, OTS 61−11400, National Science Foundation, Washington D.C., 1961.

[18] T.N. Patsios, K.V. Spiliopoulos, A force–based formulation for the 2nd order elastoplastic analysis of frames, *Proc. 2nd ECCOMAS Young Investigator's Conference*, 104–108, Bordeaux, France, September 2-6, 2013.

[19] T.N. Patsios, K.V. Spiliopoulos, A force–based formulation for the analysis of frames with non–holonomic hardening plastic hinges, *WCCM XI, ECCM V, ECFD VI*, Barcelona, Spain, July 20–25, 2014.